HSPI The Open Access Publisher

IJPRA ISSN 2766-2748 INTERNATIONAL JOURNAL OF PHYSICS RESEARCH AND APPLICATIONS

Research Article

Mirroring the Pyramidal-Neuron Cell Behavior in the Continuous-time Artificial Hopfield Neural Network. What Problems Arise?

Andreea V Cojocaru* and Stefan Balint

Department of Computer Science, West University of Timisoara, Blvd. V. Parvan 4, 300223 Timisoara, Romania

Abstract

This paper provides a mirroring of the voltage dynamics of a biological pyramidal nervous cell in the framework of the continuous-time Hopfield artificial neural network. The initial aim was to identify those elements that can explain the empirically established voltage dynamics of the biological pyramidal nervous cell. We could not achieve this desire because we encountered a major obstacle related to the current dynamics in a circuit where the capacitance is not ideal, as in the lipid bilayer of the membrane of a biological nervous cell. This phenomenon was empirically observed and mathematically described by J. Curie and von Schweidler back in the last century, but was not successfully implemented in the theory of electrical circuits. That is why we stopped at the stage "what problems arise?"

More Information

***Corresponding author:** Andreea V Cojocaru, Department of Computer Science, West University of Timisoara, Blvd. V. Parvan 4, 300223 Timisoara, Romania, Email: candreeavalentina@gmail.com

Submitted: May 27, 2026
Accepted: June 03, 2026
Published: June 04, 2026

Citation: Cojocaru AV, Balint S. Mirroring the Rosehip-neuron Cell Behavior in the Continuous-time Artificial Hopfield Neural Network. What Problems Arise? Int J Phys Res Appl. 2026; 9(6): 190-201. Available from: https://dx.doi.org/10.29328/journal.ijpra.1001156

Keywords: Peltier module; Air-water generator; Thermoelectric cooling: Water from air; Renewable water supply,; Alternative water generation; Air humidification; Water desalination

1. Introduction

In the real world, there are biological neural systems and artificial(homemade) neural systems. For the biological ones, the mathematical framework was developed by Hodgkin-Huxley (Nobel Prize in 1963), and for the artificial ones, it was developed by Hopfield (Nobel Prize in 2024). In both of these descriptions, the capacitances in the circuits that appear are ideal. This assumption has led to much debate because, in reality, the capacitances in real circuits are not ideal! The debate is not over even today! Works that try to describe the phenomenon with fractional time derivatives are not objective (they depend on the observer and are inconsistent). The aim of our paper initially was to analyze how the behavior of a neural network composed of pyramidal biological cells is reflected in a Hopfield-type artificial neural network model having ideal capacitance. This aim is not just an academic curiosity, considering the fact that measurements in the case of pyramidal biological cells are also made using artificial neural networks (circuits).

Pyramidal cells, or pyramidal neurons, are a type of multipolar neuron found in areas of the brain including the third layer of cerebral cortex, the hippocampus, and the amygdala. Pyramidal cells are the primary excitation units of the mammalian prefrontal cortex and the corticospinal tract.

One of the main structural features of the pyramidal neuron is the conically shaped soma, or cell body, after which the neuron is named. Other key structural features of the pyramidal cell are a single axon, a large apical dendrite, multiple basal dendrites, and the presence of dendritic spines [1] (Figure 1.1).

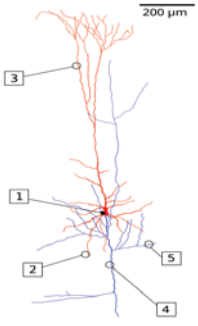

Figure 1.1: A reconstruction of a pyramidal cell. Soma and dendrites are labeled in red, axon arbor in blue. (1) Soma, (2) Basal dendrite, (3) Apical dendrite, (4) Axon, (5) Collateral axon.

Pyramidal neurons are also one of two cell types where the characteristic sign, Negri bodies, is found in post-mortem rabies infection [2]. Pyramidal neurons were first discovered and studied by Santiago Ramón y Cajal [3,4] (Figure 1.2).

Since then, studies on pyramidal neurons have focused on topics ranging from neuroplasticity to cognition.

Like dendrites in most other neurons, the dendrites are generally the input areas of the neuron, while the axon is the neuron's output. Both axons and dendrites are highly branched. The large amount of branching allows the neuron to send and receive signals to and from many different neurons.

Pyramidal neurons, like other neurons, have numerous voltage-gated ion channels. In pyramidal cells, Na+, Ca2+, and K+ channels are abundant in the dendrites and some channels in the soma [5,6]. Ion channels within pyramidal cell dendrites have different properties from the same ion channel type within the pyramidal cell soma [7,8]. Voltage-gated Ca^{2+} channels in pyramidal cell dendrites are activated by subthreshold EPSPs and by back-propagating action potentials. The extent of back-propagation of action potentials within pyramidal dendrites depends upon the K^+ channels. K^+ channels in pyramidal cell dendrites provide a mechanism for controlling the amplitude of action potentials [9].

The ability of pyramidal neurons to integrate information depends on the number and distribution of the synaptic inputs they receive. A single pyramidal cell receives about 30,000 excitatory inputs and 1700 inhibitory (IPSPs) inputs. Excitatory (EPSPs) inputs terminate exclusively on the dendritic spines, while inhibitory (IPSPs) inputs terminate on dendritic shafts, the soma, and even the axon. Pyramidal neurons can be excited by the neurotransmitter glutamate [1,10] and inhibited by the neurotransmitter GABA [1].

Pyramidal neurons have been classified into different subclasses based upon their firing responses to 400-1000 millisecond current pulses. These classifications are RSad, RSna, and IB neurons.

Figure 1.2: Santiago Ramón y Cajal. 1888.

RSad pyramidal neurons, or adapting regular spiking neurons, fire with individual action potentials (APs), which are followed by a hyperpolarizing afterpotential. The after potential increases in duration, which creates spike frequency adaptation (SFA) in the neuron [11].

RSna pyramidal neurons, or non-adapting regular spiking neurons, fire a train of action potentials after a pulse. These neurons show no signs of adaptation [11].

IB pyramidal neurons, or intrinsically bursting neurons, respond to threshold pulses with a burst of two to five rapid action potentials. IB pyramidal neurons show no adaptation [11].

Several studies are showing that morphological and electrical pyramidal cells could be deduced from gene expression measured by single-cell [12]. Several studies propose that single-cell classifications in mouse[13] and human[14] neurons based on gene expression could explain various neuronal properties. Neuronal types in these classifications are split into excitatory, inhibitory, and hundreds of corresponding subtypes. For example, pyramidal cells of layer 2-3 in humans are classified as FREM3 type [12] and often have a high amount of Ih-current [15] generated by the HCN channel.

Pyramidal neurons are the primary neural cell type in the corticospinal tract. Normal motor control depends on the development of connections between the axons in the corticospinal tract and the spinal cord. Pyramidal neurons in the prefrontal cortex are implicated in cognitive ability. Pyramidal cells within the prefrontal cortex appear to be responsible for processing input from the primary auditory cortex, primary somatosensory cortex, and primary visual cortex, all of which process sensory modalities. These cells might also play a critical role in complex object recognition within the visual processing areas of the cortex. The hippocampus's pyramidal cells are essential for certain types of memory and learning. They form synapses that aid in the integration of synaptic voltages throughout their complex dendritic trees through interactions with mossy fibers from granule cells. The interactions between pyramidal cells and an estimated 41 mossy fiber boutons, each originating from a unique granule cell, highlight the role of these boutons in information processing and synaptic connectivity, which are essential for memory and learning (Figure 1.3).

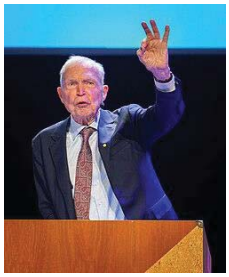

Figure 1.3: John Joseph Hopfield delivering his lecture at the 2024 Nobel Prize lectures.

Continuous-time artificial Hopfield neural networks claim to be mathematical descriptions of voltage propagation appearing in artificial neural networks. If this description is valid also for the biological nervous system, then the voltage propagation in a pyramidal nervous cell has to be mirrored with accuracy in this framework. This paper aims to identify those elements in the Hopfield artificial neural network that can explain the empirically established properties of the biological pyramidal cell.

A continuous-time Hopfield-type artificial neural network, describing the voltage evolution in an artificial network of n neurons, is a system of nonlinear differential equations of the form

$$\dot{x}_i - a_i \times x_i + \sum_{j=1}^{j=n} T_{ij} \times g_j\left(x_j\right) + I_i \quad i = 1 \ldots n \qquad (1.1)$$

where: $a_i > 0$, I_i are constants: a_i related to the neuron i membrane capacity and I_i related to the external electrical input, $T = (T_{ij})_{n \times n}$ is a constant matrix referred to as the interconnection matrix, $g_j : R \to R, j = 1 \ldots n$, represent the neuron j input-output activation function. (See [16] pg.173 formula (5.1)) An activation function g_j is a mathematical "gate" between the input feeding the neuron j and its output going to the next neuron. Decides whether neuron j should be activated or not. This means that it will decide whether the neuron's j input to the network is important or not in the process of prediction using simpler mathematical operations. The input-output activation functions are used to calculate some intermediate function in the hidden layer, which is then used to calculate an output. In the feedforward propagation, the activation function is a mathematical "gate" between the input feeding the current neuron and its output going to the next layer. In neuroscience, the input-output (I-O) activation function of a pyramidal neuron is most commonly described as a sigmoid function.

The system (1.1) can be written in matrix form:

$$\dot{X} = A \times X + T \times G(X) + I \qquad (1.2)$$

Where

$X = (x_1, x_2, \ldots, x_n)^T$, $A = diag(-a_1, -a_2, \ldots - a_n) \in M_{n \times n}$,

$I = (I_1, I_2, \ldots I_n)^T \in R^n$ and $G : R^n \to R^n$ is given by

$G(X) = (g_1(x), g_2(x), \ldots g_n(x))^T$.

Let F: $Rn \times Rn \bullet Rn$ be the function given by

$F(X, I) = A \times X + T \times G(X) + I$. With this function, equation (1.2) can be written in the form:

$$\dot{X} = F(X, I) \qquad (1.3)$$

By definition, a resting state of (1.3) is a solution of the equation:

$$F(X, 0) = 0 \qquad (1.4)$$

In other words, a resting state of the system is an element X^0 from R^n which verifies (1.4). A resting state X^0 (if exist) then X^0 is called 'rest potential.' The name 'rest potential X^0' is justified by the fact that if I is equal to 0 then the solution of (1.3) that verifies the initial condition $X(t_0) = X^0$ is constant equal to X^0. According to [16], given voltage state X is resting state if and only if it is a solution of the nonlinear algebraic equation:

$$0 = -A \times X - T \times G(X) \qquad (1.5)$$

Theoretically, it can happen that for an equation there is no solution, there exists one solution, or there exist several different voltage states, $X^j, j = 1 \ldots m$ which are solutions for (1.5).

2. Computing the transfer coefficient T and the dependence of T on the membrane time constant $\tau_m = R_m \times C_m (a = \frac{1}{\tau_m})$ in the case of a single pyramidal nervous cell, in the Hopfield artificial neural network, in the case of the sigmoid input-output activation function

For a single nervous cell, the system of differential equations (1.1) becomes

$$\dot{X} = -a \times x + T \times g(x) + I \qquad (2.1)$$

A given voltage state is a rest state if it is a solution of the next equation

$$0 = -a \times x_0 + T \times g(x_0) \qquad (2.2)$$

Therefore, for a given input-output function $g(x)$ according to (2.2), if x_0 is a rest state and $g(x_0) \neq 0$, then the transfer coefficient T corresponding to a and the rest state x_0 is given by:

$$T(a, x_0) = a \times \frac{x_0}{g(x_0)} \qquad (2.3)$$

If $g(x_0) = 0$ then according to (2.2), $x_0 = 0$. Therefore, in the case of a rest state $x_0 \neq 0$ an input –output function g for which $g(x_0) = 0$ is not appropriate. The physical reason is that there is no feedback. For this reason, in case of a rest state $x_0 \neq 0$ it is necessary to consider the input –output function g for which $g(x_0) \neq 0.$.

For the pyramidal nervous cell, the rest potential x_0 in scientific literature is estimated to be around -75 [mV] = -75 × 10^{-3} [V] and -60 [mV] = -60 × 10^{-3} [V]. The range of the values of the sigmoid input-output function $g(x) = \frac{1}{1 + e^{-x}}$ for $x \in [-0.075, -0.06][V]$ is $g(x) \in [0.4812587841, 0.4850044983]$. Therefore, the sigmoid input-output function does not vanish, $g(x) \neq 0$, for $x \in [-0.075, -0.06][V]$ and formula (2.3) can be used. According to (2.3), in the case of the pyramidal nervous cell, the transfer coefficient T is given by (2.3). On the other hand, the numerical value of the membrane time constant $\tau_m = R_m \times C_m$ for a typical pyramidal nervous cell generally falls within the range of 10 to 30 milliseconds (ms). Therefore, $a = \frac{1}{\tau_m}[s]^{-1}$

falls within the range $\frac{1}{10[ms]}=10^2[s]^{-1}$ and $\frac{1}{30[ms]}=\frac{1}{3}\times10^2[s]^{-1}$ $a\in\left[\frac{1}{3}\times10^2,10^2\right][s]^{-1.}$ By using (2.3), it is possible to compute the transfer coefficient $T(a,x_0)$ variation for $a\in\left[\frac{1}{3}\times10^2,10^2\right][s]^{-1}$ and $x_0\in[-0.075,-0.06]$ [V]. In case of the so called 'Sigmoid/ Logistic' input-output function $g(x)=$, and for two fixed values of the rest potentials $x_0=-75[mV]=-75\times10^{-3}$[V] $x_0=-60\ [mV]=60\times10^{-3}[V]$ the transfer coefficients variations $T(a,x_0)$ as functions of $a\in[\frac{1}{3}\times10^2,\ 10^2][s]^{-1}$ are presented on the next Figures 2.1, 2.2, 2.3:

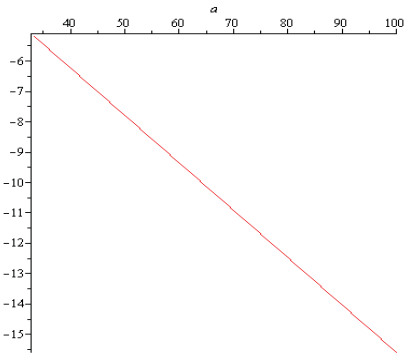

Figure 2.1: . T (a ∈ [1/3 ×10², 10²] [s⁻¹].

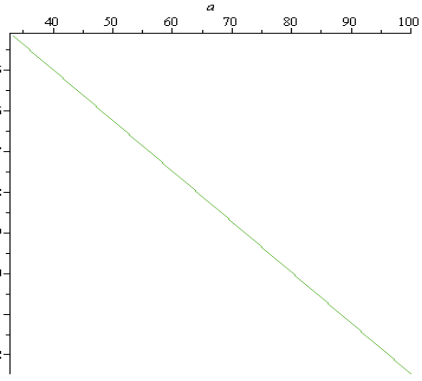

Figure 2.2: T (a, - 0.06), a ∈ [1/3 × 10², 10²] [s]⁻¹.

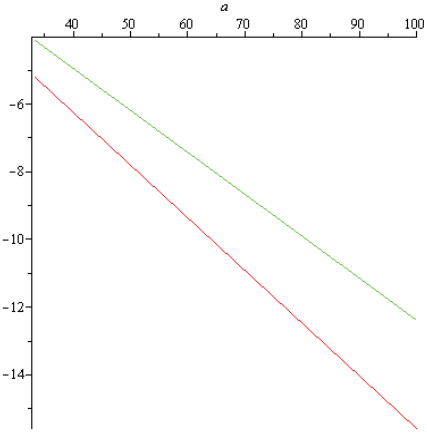

Figure 2.3: (a, - 0.075), red T (a, - 0.06), green aє [1/3 ×10², 10²] [s⁻¹].

The labels on the vertical axis are missing because T is a number (transfer coefficient) without physical dimension.

In this context, the sign minus physical meaning is 'negative feedback' (self-inhibition). It is related to instability. If T is negative, the rest state is unstable, i.e., the pyramidal cell voltage is no longer an energy minimum. The cell state tends to "run away" from the current state.

For the two remaining states $x_0=-75\times10^{-3}[V]$ and $x_0=-60\times10^{-3}[V]$ and for two values of capacitance 'a'; 'a'; $a=10^2[s]^{-1}$ and $a=\frac{1}{3}\times10^2[s]^{-1.}$ and this kind of dynamics is represented with red and green colors respectively, on the next figures 2.4, 2.5:

The conclusions, obtained by computation, in this section can be summarized as follows:

-formula $T(a,x_0)=a\times\frac{x_0}{g(x_0)}$ is an explicit functional relationship between the transfer coefficient T, the 'membrane capacity a 'and the sigmoid input-output function $g(x)=\frac{1}{1+e^{-x}}$ value at the rest voltage -75×10^{-3}[V], and -60×10^{-3} respectively. The values of these transfer coefficients are:

$T(10^2,-0.075)=-15.5841311$, $T(\frac{1}{3}\times10^2,-0.075)=-5.194710378$ = , $T(10^2,-0.06)=-12.37101928$,

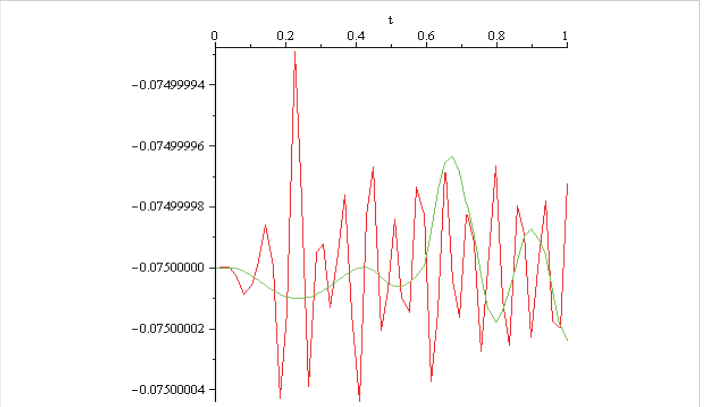

Figure 2.4: x_0=-75×10⁻³ [V], a = 10² [s]⁻¹ red, a = 1/3×10² [s]⁻¹ green.

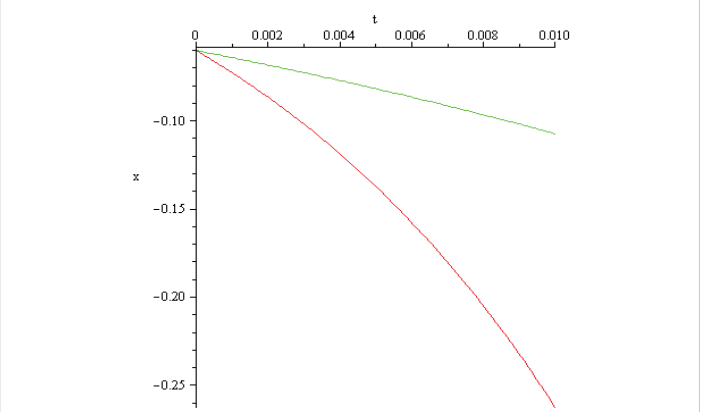

Figure 2.5: x_0=-60×10⁻³ [V], a=10²[s]⁻¹ red, a = 1/3×10² [s]⁻¹ green.

$$T(\frac{1}{3}\times 10^2, -0.06) = -4.123673094$$

-The transfer coefficients variations $T(a, x_0)$ as functions of $a \in [\frac{1}{3}\times 10^2,\ 10^2][s]^{-1}$, are negatives. In this context, the sign minus has physical meaning as negative feedback (self-inhibition). It is related to instability. If $T(a, x_0)$ is negative, the rest state is unstable, i.e., the pyramidal cell voltage is no longer an energy minimum. The cell state tends to "run away" from the current state.

-the dynamic of the rest state

$x_0 = -75\times 10^{-3}[V]$, *for* $a = 10^2[s]^{-1}$ *and* $a = \frac{1}{3}\times 10^2[s]^{-1}$

is oscillatory.

-the dynamic of the rest state

$x_0 = -60\times 10^{-3}[V]$ for $a = 10^2[s]^{-1}$ *and* $a = \frac{1}{3}\times 10^2[s]^{-1}$, is decreasing.

3. Mirroring, the first stage (i.e., rest potential of $-75\times 10^{-3}[V]$ evolves toward threshold potential of $-0.055[V]$) dynamics, in the Hopfield artificial neural network using the sigmoid input-output activation function. Dynamic dependence on the membrane time constant $\tau_m = R_m \times C_m$ $(a = \frac{1}{\tau_m})$, in the case of a single pyramidal nervous cell

The resting potential is the difference in electrical charge (voltage) between the inside and outside of a pyramidal nervous cell when it is not stimulated. It is a state of polarization, with the inside negative relative to the outside, usually in the range -75 [mV] and - 60 [mV], maintained by ion pumps and the selective permeability of the membrane (Figures 3.1, 3.2).

The Nobel Prize in Physiology or Medicine 1963 was awarded jointly to Sir John Carew Eccles, Alan Lloyd Hodgkin, and Andrew Fielding Huxley for their discoveries concerning the ionic mechanisms involved in excitation and inhibition in the peripheral and central portions of the nerve cell

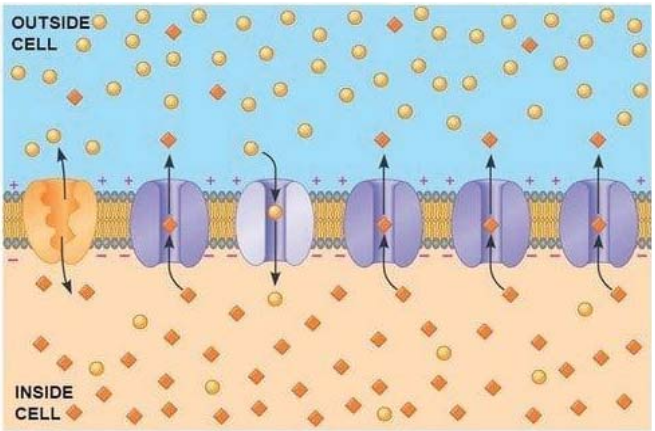

Figure 3.1: Pyramidal nervous cell membrane.

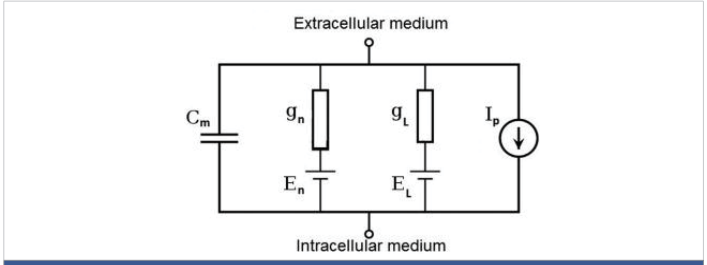

Figure 3.2: Hodgkin-Huxley electrical circuit model of the biological nervous cell for voltage dynamics.

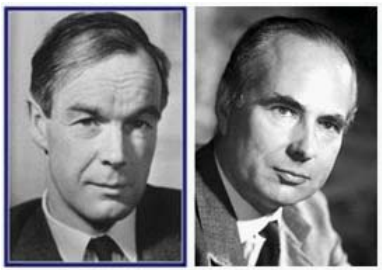

membrane. The typical Hodgkin–Huxley [17] model treats each component of an excitable cell as an electrical element (as shown in the figure). The lipid bilayer is represented as a capacitance (C_m). Voltage-gated ion channels are represented by conductances (g_n, where n is the specific ion channel) that depend on both voltage and time. Leak channels are represented by linear conductances (g_L). The electrochemical gradients driving the flow of ions are represented by voltage sources (E_n) whose voltages are determined by the ratio of the intra- and extracellular concentrations of the ionic species of interest. Finally, ion pumps are represented by current sources (I_p). The membrane potential is denoted by V_m. Mathematically, the current flowing into the capacitance of the lipid bilayer is written as

$$I_c = C_m \frac{dV_m}{dt} \quad (3.1)$$

and the current through a given ion channel is the product of that channel's conductance and the driving potential for the specific ion

$$I_i = g_i(V_m - V_i) \quad (3.2)$$

where V_i is the reversal potential of the specific ion channel. Thus, for a cell with sodium and potassium channels, the total current through the membrane is given by:

$$I = C_m \frac{dV_m}{dt} + g_K(V_m - V_K) + g_{N_a}(V_m - V_{N_a}) + g_h(V_m - V_h) \quad (3.3)$$

Using a series of voltage clamp experiments and by varying extracellular sodium and potassium concentrations, Hodgkin and Huxley developed a model in which the properties of an excitable cell are described by a set of four ordinary differential equations. Together with the equation for the total current mentioned above, these are:

$$I = C_m \frac{dV_m}{dt} + \bar{g}_k\ n^4(V_m - V_K) + \bar{g}_{N_a} m^3(V_m - V_{N_a}) + \bar{g}_h(V_m - V_h)$$

$$\frac{dn}{dt} = \alpha_n(V_m)(1-n) - \beta_n(V_m)n$$

$$\frac{dm}{dt}=\alpha_m(V_m)(1-m)-\beta_m(V_m)m \tag{3.4}$$

$$\frac{dh}{dt}=\alpha_h(V_m)(1-h)-\beta_h(V_m)h$$

where I is the current per unit area and α_i and β_i are rate constants for the i-th ion channel, which depend on voltage but not time. $\overline{gk}$, $\overline{gn_a}$, $\overline{gl}$ is the maximal value of the conductance. n, m, and h are dimensionless probabilities between 0 and 1 that are associated with potassium channel subunit activation, sodium channel subunit activation, and sodium channel subunit inactivation, respectively.

For instance, given that potassium channels in squid giant axon are made up of four subunits, which all need to be in the open state for the channel to allow the passage of potassium ions, the n needs to be raised to the fourth power. For $p=(n,m,h)$, a_p and β_p take the form

$$\alpha_p(V_m)=p_\infty(V_m)/\tau_p \tag{3.5}$$

$$\beta_p(V_m)=1-p_\infty(V_m)/\tau_p \tag{3.6}$$

p_∞ and $1-p_\infty$ are the steady-state values for activation and inactivation, respectively, and are usually represented by Boltzmann equations as functions of V_m.

This model, conceived for one biological nervous cell, was extended for a network of biological nervous cells [18]. Due to the discrepancy between the computed and measured data, besides the integer-order derivatives, the temporal fractional order derivative was introduced in the model [18]. The consequence was that the model became nonobjective [19].

Comparing the mathematical description defined by equations (3.4) with that defined by equations (2.1), we note that in the case of description (2.1), the consequences of opening and closing the gates must be described by changing the values of the external input current in (2.1).

The action potential is a rapid, temporary change in the pyramidal membrane potential, whereby the inside becomes positive relative to the outside. First, the pyramidal nervous cell receives external input, which opens the Na+ sodium channels. If the Na+ influx is large enough to raise the membrane potential from [-75, -60] [mV] to about [-50, -45] [mV], the threshold value, the "event" is triggered. Once the threshold is reached, the voltage-gated sodium channels open massively. Na+ ions rush into the cell, and the interior suddenly becomes positive up to +20 [mV] or +40 [mV].

For a pyramidal nervous cell, to fire an action potential, an incoming current must cause the membrane potential to depolarize from its resting potential, which is in the range [-75, -60] [mV], into the threshold potential, which is in the range [-55, -45] [mV].

In literature, there is no single specific value for an input current that applies to all nervous cells for depolarization; the required current varies.

Depending on the neuron's type, size, and the desired outcome, but it is typically measured in pico-amperes 10^{-12} $[A]$ or nano- amperes 10^{-9} $[A]$.

In the continuous time Hopfield artificial neural network model the pyramidal cell voltage dynamics presented is governed by the solution of one of the boundary value problems:

$$\dot{x}=-a\times x+T\times g(x)+I \tag{3.7}$$

$$x(0)=-0.075,\ x(0.15)=-0.055 \tag{3.8}$$

$$x(0)=-0.06,\ x(0.15)=-0.045 \tag{3.9}$$

Formulas (3.7), (3.8), (3.9) define two different boundary value problems in case of the same equation. (3.7), (3.8) is the first, and (3.7), (3.9) is the second.

Solving numerically the boundary value problems (3.7), (3.8) and (3.7), (3.9) for $a=10^2[s]^{-1}$ and $a=\frac{1}{3}\times10^2[s]^{-1}$, $g(x)=\frac{1}{1+e^{-x}}$ and transfer coefficients, $T(10^2,-0.075)=-15.58413113$, $T(10^2,-0.06)=-12.37101928$, $T(\frac{1}{3}\times10^2,-0.075)=-5.194710378=$, $T(\frac{1}{3}\times10^2,-0.06)=-123673094=$ it is possible to find the value of the external impulse value I which lends one of the rest states $x(0)=-0.075$, $x(0)=-0.06$, into a threshold value in the range $[-0.055,-0.045][V]$.

Taking for cortical pyramidal neurons the rest voltage $-0.075[V]$, the threshold potential voltage $-0.055[V]$ (i.e. the voltage at which voltage-gated sodium channels open to initiate an all-or-none spike), and a time frame $0.15[s]$ for this process we find by computation that ir case of the transfer coefficient, $T(10^2,-0.075)=-15.58413113$, the external input value is I = 2$[A]$ and in case of the transfer coefficient $T(\frac{1}{3}\times10^2,\ -0.075)=-5.194710378$, the external input value is I = 069$[A]$. The computed voltage dynamics is presented in the next Figure 3.3:

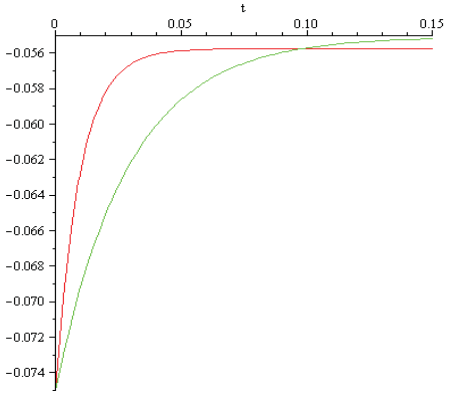

Figure 3.3: a = 10² [s]⁻¹, x_0=-0.075[V], x_1=-0.055[V], I_1= 2[A], color red; a = 10²/3 [s]⁻¹, x_0 = -0.075[V], x_1 = -0.055[V], I_1 = 0.69[A] color green.

Taking for layer 5 pyramidal neurons the rest voltage $-0.06[V]$, the threshold voltage $-0.045[V]$ (i.e. the voltage at which voltage-gated sodium channels open to initiate an all-or-none spike), and a time frame of $0.15[s]$ for this process, using the transfer coefficient, $T(10^2,-0.06)=-12.37101928$, we find by computation that, the external input value is $I = 1.5[A]$, and in case of the transfer coefficient $T(\frac{1}{3}\times 10^2,-0.06)=-4.123673094$, we find by computation that, the external input value is $I = 0.52[A]$. The computed voltage dynamic is presented in the next Figure 3.4:

The magnitude of the input currents obtained in these computations differs extremely much from those discussed in literature (order of magnitude nano or pico amperes). Therefore, boundary value problems (3.7), (3.8) and (3.7), (3.9) doesn't mirror correctly the reality. The 'explanation' of this discrepancy could be the Curie-von Sweidler law appearing in dielectric (i.e.in the double lipid layer of the cell membrane). Curie–von Schweidler law: refers to the response of dielectric material to the step input of a direct current (DC) voltage first observed by Jacques Curie [20,21] and Egon Ritter von Schweidler [22]. The Curie current represents the response of adielectric material to a step input DC voltage. According to [20,21].

the curie current intensity is given by

$$i_{Curie}(t)=V_0\times\frac{t^{-\alpha}}{h} \tag{3.10}$$

In [22] von Schweidler presents the main forms of abnormal behavior of dielectrics as follows.If the terminals of a capacitor are connected to the poles of a current source with constant electromotive force, a current will appear in the conductors, the intensity of which decreases with time. For an ideal non-conducting dielectric, according to the general theory, the following differential equation applies to the "normal charging current":

$$L\times\frac{d^2i}{dt^2}+R\times\frac{di}{dt}+\frac{1}{C}\times i=0 \tag{3.11}$$

where C is the capacitance of the capacitor, L the self-inductance coefficient, and R the resistance of the external circuit. Depending on the ratio of the numerical values of these three constants, the charging of the capacitor occurs either oscillatory or aperiodically. With a relatively small resistance of the external circuit, the current in each of the two traps decreases very rapidly, so that in practically realizable traps the normal charging current can be set to zero after times of the order of a small fraction of a second.

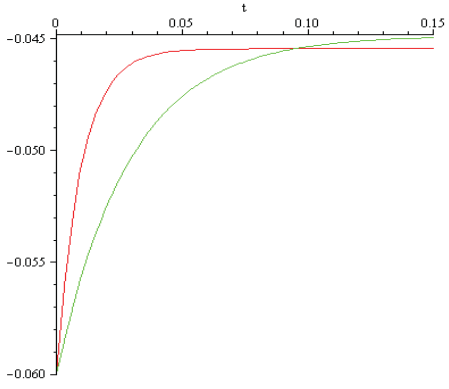

Figure 3.4: $a = 10^2\,[s]^{-1}$, $x_0 = -0.06[V]$, $x_1 = -0.045[V]$, $I_1 = 1.5[A]$, color red; $a = 10^2/3\,[s]^{-1}$, $x_0 = -0.06[V]$, $x_1 = -0.045[V]$, $I_1 = 0.52[A]$ color green.

If the dielectric is not perfectly insulating, then a normal conduction current 'a' is superimposed on the normal charging current, 'a' is given by the formula

$$a=\frac{4\times\pi\times\lambda}{K}\times C\times E \tag{3.12}$$

where λ is the specific conductance, K is the dielectric constant of the medium, C is the capacitance of the capacitor and E is the electromotive force of the current source (all quantities are considered to be measured in absolute electrostatic units).

In fact, as can be seen, in many dielectrics, besides the normal charging current and the normal conduction current, there is another "anomalous charging current" that overlaps, so that the entire current can be represented by:

$$J_1=i_1+y_1+a \tag{3.13}$$

Here, γ_1 is a function of time that asymptotically decreases to zero, but it is much more complex than the normal load current i_1.

If the terminals of the capacitor are connected together after being maintained at a constant potential difference for a time interval δ, then two Open must be distinguished in terms of the laws of the discharge current:

a). The discharge current J_2 corresponds to the normal discharge current i_2, which is determined by an analogous integer differential equation, like the normal load current i_1;

b) Analogous to the load, an "anomalous discharge current" γ_2 is superimposed, and γ_2 is again a function of it that decreases to zero with increasing time. The following relationship between γ_1 and γ_2 is also valid:

$$\int_0^{\delta} y_1dt=-\int_0^{\infty} y_2dt \tag{3.14}$$

That is, the total amount of electricity passing through a cross section of the conductor as a result of the abnormal discharge current is equal to the amount that was carried by the abnormal charge current during the charging period δ.

In case a), which is carried out especially with various poorly conductive liquids (Koller; Schweidler; Gadeke), the charging process proceeds as if the conductivity of the medium were undergoing temporal changes due to the passage of current.

In case b), the charging process is reversible; the medium

behaves as if the conductivity corresponding to the time integral of the abnormal charging current $\int_0^{\delta} y_1 dt$. The amount of electricity absorbed is gradually released again during the discharge. This reversible process is usually referred to as the formation or pre-production of the "residue", and the integral $\int_0^{\delta} y_1 dt$ as the "residual charge" formed during time δ.

In principle, the situation is less simple when the capacitor terminals are not held at constant potentials, but one of them is isolated; however, this form of residual phenomenon is historically the main one and this has led to the aforementioned name. If a capacitor is charged and then one of the two terminals is isolated, the potential difference V between the terminals, and therefore the so-called "dissipative charge" given by the product CV, decreases. This decrease occurs more rapidly than would correspond to the constant conduction current '*a*'. Conversely, if the charged capacitor is discharged by temporarily connecting the terminals and only one terminal is isolated, a new charge of the same sign as the original gradually appears, increases to a maximum and then (due to the conduction of the dielectric) decreases asymptotically to zero. Regarding the laws that apply to the temporal evolution of residual phenomena and their dependence on other constraints, experimental investigations have led to the following results:

The anomalous charging current or residue formation current γ_1, at the terminals of a given capacitor with a given electromotive force, can be represented as a function of time by:

$$y_1 = B \times t^{-n} \quad 0 < n < 1 \tag{3.15}$$

This formula can only be considered an approximation, because initially, we obtain for t = 0, $\gamma_1 = \infty$. This means that equation (3.1) with '*a*' constant is not appropriate for the description of real phenomenon. For more detail see [21], [22].

The main conclusion, obtained by computation, in this section can be summarized as follows:

-The magnitude of the input currents obtained in these calculations differs extremely much from those discussed in literature (order of magnitude nano or pico amperes). Therefore, boundary value problems (3.7),(3.8) and (3.7),(3.9) doesn't mirror correctly the reality in the first stage of the activation potential. The 'explanation' of this discrepancy could be the ignorance of Curie-von Sweidler law appearing in dielectric (i.e.in the double lipid layer of the cell membrane).

4. Mirroring, the voltage dynamics, in the second stage (i.e. threshold potential of -55 × 10^{-3}[V] evolve toward spike potential of +0.01[V] or threshold potential of -0.06[V] evolve toward -0.045[V]), in Hopfield artificial neural network, by using the sigmoid input-output activation function. Dynamics dependence on the membrane time constant τm = Rm Cm $(a = \frac{1}{\tau_m})$ in case of a single pyramidal nervous cell

If the Na+ influx is large enough, to raise the rest membrane potential, of [-0.075, -0.060] [V] to the threshold potential of [-0.055 – 0.045] [*V*], then the "event" is triggered. In order to describe mathematically the phenomena: "Once the threshold is reached, the voltage-gated sodium channels open massively. Na+ ions rush into the cell, and the interior suddenly becomes positive up to [0.01, 0.04] [V]".

The effect of the massive opening of sodium channels and that of the Na+ ions rush into the cell, in the framework of the Hopfield artificial neural network, we describe as the solution of the boundary value problems

$$\dot{x} = -a \times x + T \times g(x) + I \tag{4.1}$$

$$x(0) = -0.055,\ x(0.15) = 0.01 \tag{4.2}$$

$$x(0) = -0.045,\ x(0.15) = 0.01 \tag{4.3}$$

Namely:

-in case $T(10^2, -0.075), I = 2[A]$, increase the exterior input in the cell from 2[A] to 9[A].

-in case $T\left(\frac{1}{3} \times 10^2, -0.075\right), I = 0.69[A]$, increase the exterior input in the cell from 0.69[A] to 3[A].

-in case $T(10^2, -0.06), I = 1.5[A]$, increase of the exterior input in the cell from 1.5[A] to 2[A].

-in case $T\left(\frac{1}{3} \times 10^2, -0.06\right), I = 0.53[A]$, increase the exterior input in the cell from 0.53[A] to 1[A].

The computed results are represented in the next Figures 4.1, 4.2:

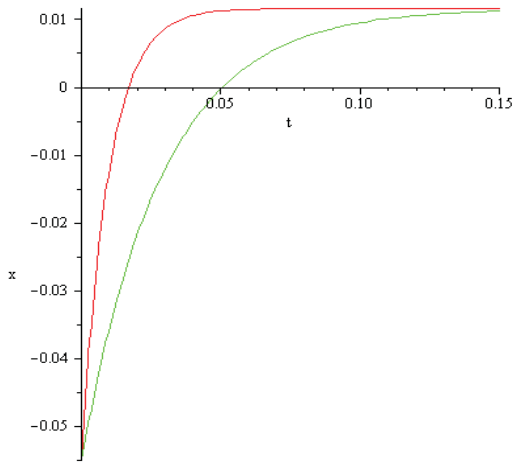

Figure 4.1: $a = 10^2$ [s]$^{-1}$, $x_1 = -0.055$[V], $x_2 = 0.01$[V], $I_2 = 9$[A], color red; $a = 10^2/3$[s]$^{-1}$, $x_1 = -0.055$[V], $x_2 = 0.01$[V], $I_2 = 3$[A] color green.

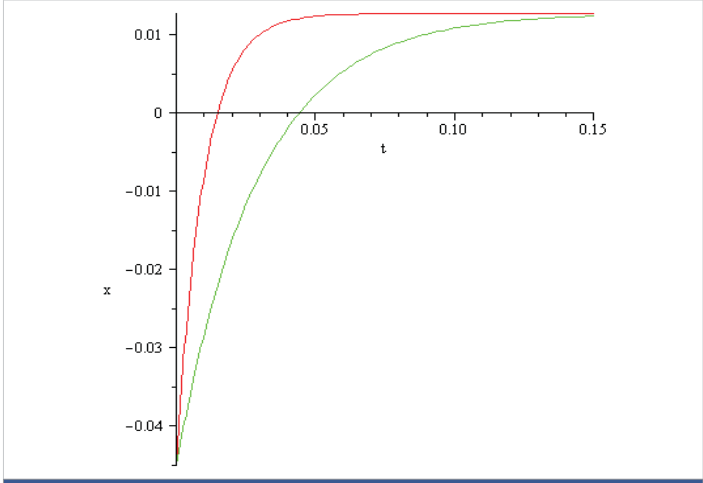

Figure 4.2: $a = 10^2$ [s]$^{-1}$, $x_1 = -0.055$[V], $x_2 = 0.01$[V], $I_2 = 9$[A], color red; $a = 10^{2/3}$[s]$^{-1}$, $x_1 = -0.055$[V], $x_2 = 0.01$[V], $I_2 = 3$[A] color green.

The main conclusion, obtained by computation, in this section can be summarized as follows:

-It is possible to mirror the voltage increase but the magnitude of the input currents obtained in computations differs extremely much from those discussed in literature (order of magnitude $10^{-9} - 10^{-12}$ [A]). Therefore, the boundary value problems (4.1), (4.2) and (4.1), (4.3) doesn't mirror correctly the reality in the second stage of activation potential, termed triggering. The 'explanation' of this discrepancy could be that the Curie-von Sweidler current appearing in dielectric (i.e.in the double lipid layer of the cell membrane) is ignored.

5. Mirroring voltage dynamics in the third stage i.e. spike potential of +0.01[V] evolves toward hyperpolarization of -0.077 [V], after that the spike potential is reached

Concerning the process dynamics, as soon as the peak +0.01 [V] of the action potential is reached, the cell must "reset" itself. Sodium channels close rapidly, potassium channels (K+) open, potassium ions leave the cell, carrying the positive charge out, and the interior of the cell becomes negative again. For a brief moment, the cell potential becomes -0.077 [V] a little more negative than normal i.e. in the range [-0.075, -0.06] [V] (hyperpolarization). At this stage, the pyramidal neuron cannot fire another impulse, which ensures that the signal travels in only one direction (forward, down the axon) and does not return. The negative depolarization potential (or negative after potential) represents the phase after reaching the peak of the action potential, when the membrane potential remains for a short period, 40-50 [ms] less negative than the rest potential, but still negative, before returning completely to the rest state.

The effect of the sodium channels close, and opening of potassium channels (K+) in the framework of Hopfield artificial network we describe as the solution of the boundary value problem

$$\dot{x} = -a \times x + T \times g(x) + I \tag{5.1}$$

$$x(0) = 0.01,\ x(0.15) = -0.077 \tag{5.2}$$

Namely:

-in case $T\left(10^2, -0.075\right), I = 9[A]$ decrease of the exterior input in the cell from 9[A] to -0.380[A].

-in case $T\left(\frac{1}{3}\times 10^2, -0.075\right), I = 3[A]$, decrease of the exterior input in the cell from 3[A] to -0.11[A].

-in case $T\left(10^2, -0.06\right), I = 1.5[A]$ decrease of the exterior input in the cell from 1.5[A] to -1.89[A].

-in case $T\left(\frac{1}{3}\times 10^2, -0.06\right), I = 0.53[A]$, decrease the exterior input in the cell from 0.53[A] to -0.65[A].

The computed results are represented in the next Figures 5.1,5.2:

The main conclusion, obtained by computation, in this section can be summarized as follows:

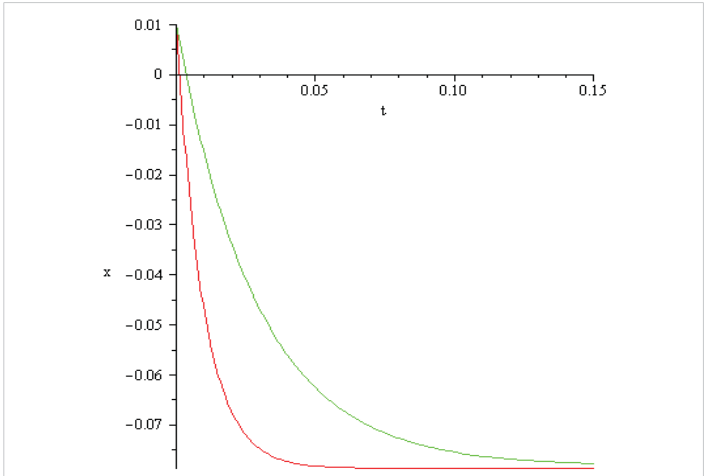

Figure 5.1: $a = 10^2$ [s]$^{-1}$, $x_2 = 0.01$[v], $x_3 = -0.077$[V], $I_3 = -0.380$[A], color red; $a = 10^{2/3}$ [s]$^{-1}$, $x_2 = 0.01$[V], $x_3 = -0.077$[V], $I_2 = -0.11$[A] color green.

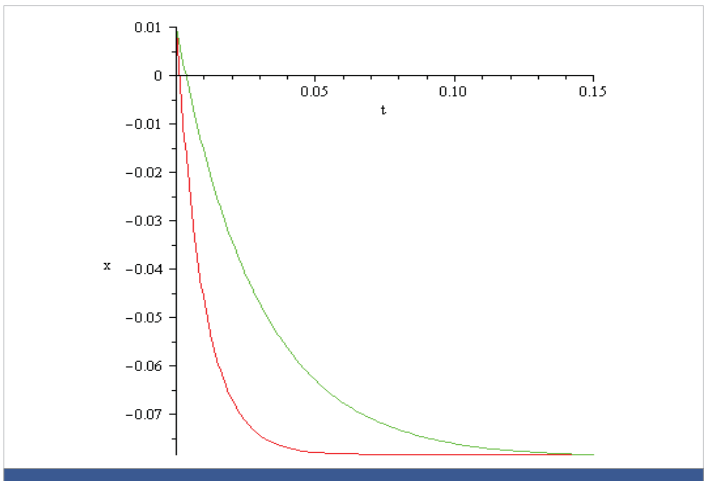

Figure 5.2: $a = 10^2$ [s]$^{-1}$, $x_2 = 0.01$[v], $x_3 = -0.077$[V], $I_3 = -1.89$[A], color red; $a = 10^{2/3}$ [s]$^{-1}$, $x_2 = 0.01$[V], x3 = -0.077[V], $I_3 = -0.65$[A] color green.

It is possible to mirror the voltage decrease but the magnitude of the input currents obtained in computations differs extremely much from those discussed in literature (order of magnitude $10^{-9} - 10^{-12}$ [A]). Therefore, boundary value problem (5.1), (5.2) doesn't mirror correctly the reality in the third stage of activation potential termed hyperpolarization. The 'explanation' of this discrepancy could be that the Curie-von Sweidler current appearing in dielectric, i.e.in the double lipid layer of the cell membrane, is ignored.

6. Mirroring voltage dynamics in the fourth stage, i.e. hyperpolarization of -0.077[V] evolves toward the rest state of -0.075[V] or -0.06[V]

In order to describe mathematically the dynamics of voltage during the return process from the hyperpolarization voltage of -0.077[V] to the rest voltage -0.075[V] or -0.06 [V] in 0.04-0.05 [s] the following boundary value problems were solved:

$$\dot{x} = -a \times x + T \times g(x) + I \tag{6.1}$$

$$x(0) = -0.077,\ x(0.05) = -0.075 \tag{6.2}$$

$$x(0) = -0.077,\ x(0.05) = -0.06 \tag{6.3}$$

and the following results were obtained:

- in case $T\left(10^2, -0.075\right), I = -3.80[A]$ increase of the exterior input in the cell from -3.80[A] to +0.001[A].

- in case $T\left(\frac{1}{3}\times 10^2, -0.075\right), I = -0.11[A]$, increase of the exterior input in the cell from -0.11[A] to +0.014[A].

- in case $T\left(10^2, -0.06\right), I = -1.89[A]$ increase of the exterior input in the cell from -1.89[A] to +0.001[A].

- in case $T\left(\frac{1}{3}\times 10^2, -0.06\right), I = -0.65[A]$, increase the exterior input in the cell from -0.65[A] to +0.1[A].

The computed results are represented in the next Figures 6.1,6.2:

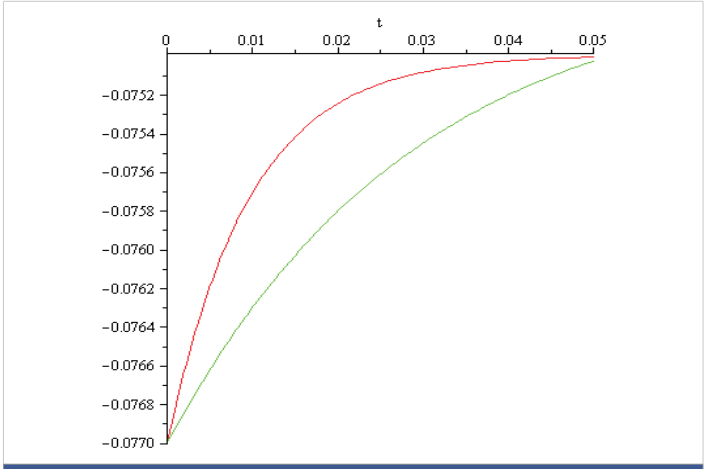

Figure 6.1: $a = 10^2$ [s]$^{-1}$, $x_3 = -0.077$[V], $x_4 = -0.075$[V], $I_4 = 0.001$[A], color red; $a = 10^{2/3}$ [s]$^{-1}$, $x_3 = -0.077$[V], $x_4 = -0.075$[V], $I_4 = 0.014$[A] color green.

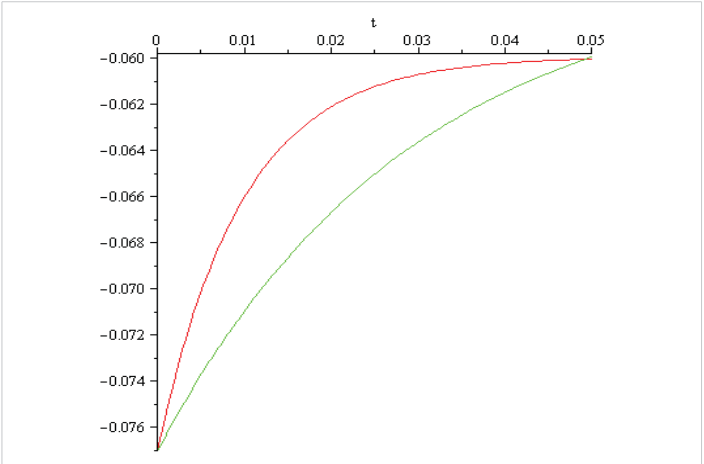

Figure 6.2: $a = 10^2$ [s]-1, $x_3 = -0.077$[V], $x_4 = -0.06$[V], $I_4 = 0.001$[A], color red; $a = 10^{2/3}$ [s]$^{-1}$, $x_3 = -0.077$[V], $x_4 = -0.06$[V], $I_4 = 0.1$[A] color green.

The main conclusion, obtained by computation, in this section can be summarized as follows:

- It is possible to mirror the voltage increase but the magnitude of the input currents obtained in these computations differs extremely much from those discussed in literature (order of magnitude $10^{-9} - 10^{-12}$ [A]). Therefore, boundary value problems (6.1), (6.2) and (6.1), (6.3) doesn't mirror correctly the reality in the fourth stage of activation potential termed return to the rest. The 'explanation' of this discrepancy could be that the Curie-von Sweidler current appearing in dielectric (i.e.in the double lipid layer of the cell membrane) is ignored.

7. Mirroring voltage dynamics of two successive oscillations of a pyramidal biological nervous cell in Hopfield artificial network, using the sigmoid input-output activation function

According to the physical description and the above computations the mirroring, in the framework of the artificial Hopfield neural network, the voltage dynamics of a pyramidal biological nervous cell is oscillatory. One oscillation is composed from fifth steps (stages).

The first step (stage) is the voltage increase from the value of the rest voltage to the value of the threshold voltage.

The second step (stage) is the increase of the voltage from the value of the threshold voltage to the value of the spike voltage.

The third step (stage) is the decrease of the voltage from the value of the spike voltage to the value of the hyperpolarization voltage.

The fourth step (stage) is the retour from the hyperpolarization voltage to the rest voltage.

The fifth step (stage) is the rest voltage.

Two successive oscillations obtained by computation are presented in the following cases:

Rest – 0.075[V], threshold – 0.055[V], $a = 10^2$, $T = -15.58413113$

ii.) Rest – 0.075[V], threshold – 0.055[V], $a = \frac{1}{3}10^2$, $T = -5.194710348$

The main conclusion, obtained by computation, in this section can be summarized as follows:

-The magnitude of the input currents obtained in these computations differs extremely much from those discussed in literature (order of magnitude 10^{-9} – 10^{-12} [A]. Therefore, the continuous artificial Hopfield the reality. The 'explanation' of this discrepancy could be the Curie-von Sweidler law appearing in dielectric (i.e.in the double lipid layer of the cell membrane) which is ignored (Figure 7.1,7.2).

Results

This paper, provide a mirroring of the voltage dynamics of a pyramidal nervous cell in the framework of continuous-time Hopfield neural network. The first part of paper is focused on the case of a single pyramidal neuron cell for which the existence, uniqueness and properties of the coefficient of the matrix transfer is found in case of the sigmoid input-output activation function. It is shown that, the magnitude of the input-output currents, corresponding to different stages of the pyramidal nervous cell, computed in the Hopfield artificial neural network, differs extremely much from those discussed in literature. The 'explanation' of this discrepancy could be the Curie-von Sweidler law appearing in dielectric (i.e.in the double lipid layer of the cell membrane), ignored in Hopfield artificial network model. The problem is moor general. In real circuits the capacities are never ideal! Even in case of artificial (homemade) networks. This phenomenon was empirically observed and mathematically described by J. Curie and von Schweidler back in the last century, but was not successfully implemented in the theory of electrical circuits.

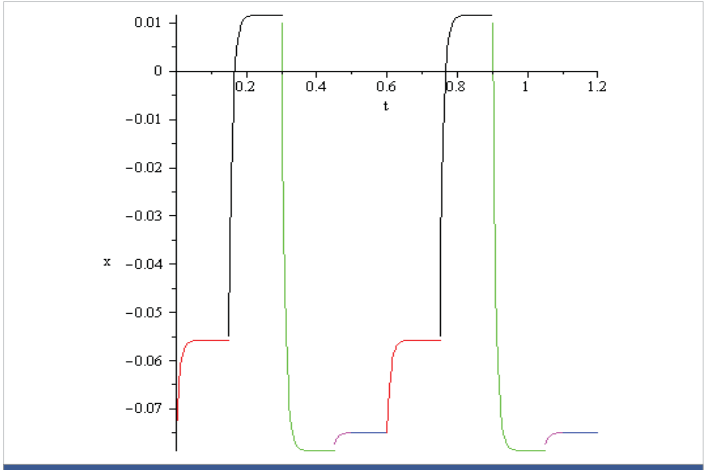

Figure 7.1: Two oscillations in the case -0.075[V], $a = {}_{1/3}\,10^2$, $T = -15.58413113$.

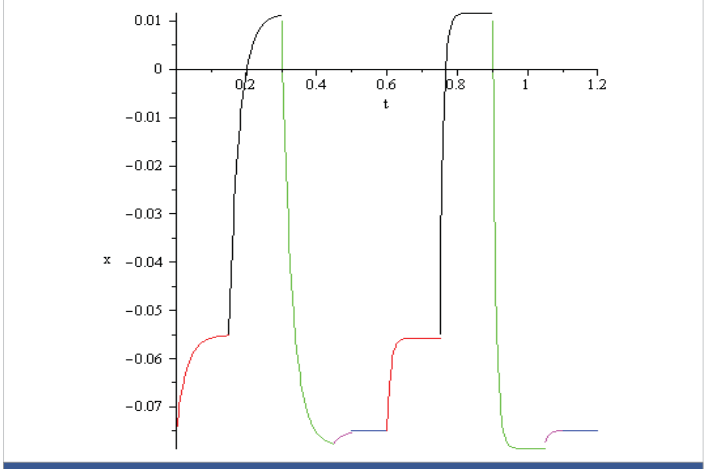

Figure 7.2: Two oscillations in the case -0.075[V], $a = 1/3\ 10^2$, $T = -5.19710348$.

The ideal capacity assumption has led to much debate. The debate is not over even today! Works that try to describe the phenomenon with fractional time derivatives are not objective (they depend on the observer and are inconsistent). That is why we stopped at the stage "what problems arise?"

Authors' Contribution: The authors contributed equally to the realization of this work. All authors have read and agreed to the published version of the manuscript.

Founding: This research did not receive any specific grant from funding agencies in the public, commercial, or not-for-profit sectors.

Data Availability Statement: The original contributions presented in the study are included in the article; further inquiries can be directed to the corresponding author.

References

1. Megías M, Emri Z, Freund TF, Gulyás AI. Total number and distribution of inhibitory and excitatory synapses on hippocampal CA1 pyramidal cells. Neuroscience. 2001;102(3):527-40. Available from: https://dx.doi.org/10.1016/S0306-4522(00)00496-6.
2. Sketchy Group, LLC. 2.3 rhabdovirus. SketchyMedical. Archived from the original on 2017 Apr 13.
3. Elston GN. Cortex, cognition and the cell: new insights into the pyramidal neuron and prefrontal function. Cereb Cortex. 2003 Nov;13(11):1124-38. Available from: https://dx.doi.org/10.1093/cercor/bhg093.
4. García-López P, García-Marín V, Freire M. Three-dimensional reconstruction and quantitative study of a pyramidal cell of a Cajal histological preparation. J Neurosci. 2006 Nov;26(44):11249-52. Available from: https://dx.doi.org/10.1523/JNEUROSCI.3543-06.2006
5. Spruston N. Pyramidal neurons: dendritic structure and synaptic integration. Nat Rev Neurosci. 2008 Mar;9(3):206-21. Available from: https://dx.doi.org/10.1038/nrn2286
6. Georgiev DD, Kolev SK, Cohen E, Glazebrook JF. Computational capacity of pyramidal neurons in the cerebral cortex. Brain Res. 2020 Dec;1748:147069. Available from: https://dx.doi.org/10.1016/j.brainres.2020.147069.
7. Golding NL, Mickus TJ, Katz Y, Kath WL, Spruston N. Factors mediating

powerful voltage attenuation along CA1 pyramidal neuron dendrites. J Physiol. 2005 Oct;568(Pt 1):69-82. Available from: https://dx.doi.org/10.1113/jphysiol.2005.086793

8. Remy S, Beck H, Yaari Y. Plasticity of voltage-gated ion channels in pyramidal cell dendrites. Curr Opin Neurobiol. 2010 Aug;20(4):503-9. Available from: https://dx.doi.org/10.1016/j.conb.2010.06.006

9. Magee J, Hoffman D, Colbert C, Johnston D. Electrical and calcium signaling in dendrites of hippocampal pyramidal neurons. Annu Rev Physiol. 1998;60:327-46. Available from: https://dx.doi.org/10.1146/annurev.physiol.60.1.327.

10. Wong RKS, Traub RD. NETWORKS | Cellular properties and synaptic connectivity of CA3 pyramidal cells: mechanisms for epileptic synchronization and epileptogenesis. In: Schwartzkroin PA, ed. Encyclopedia of Basic Epilepsy Research. Oxford: Academic Press; 2009. p.815-9. Available from: https://dx.doi.org/10.1016/b978-012373961-2.00215-0.

11. Franceschetti S, Sancini G, Panzica F, Radici C, Avanzini G. Postnatal differentiation of firing properties and morphological characteristics in layer V pyramidal neurons of the sensorimotor cortex. Neuroscience. 1998 Apr;83(4):1013-24. Available from: https://dx.doi.org/10.1016/S0306-4522(97)00463-6.

12. Berg J, Sorensen SA, Ting JT, Miller JA, Chartrand T, Buchin A, et al. Human neocortical expansion involves glutamatergic neuron diversification. Nature. 2021 Oct;598(7879):151-8. Available from: https://dx.doi.org/10.1038/s41586-021-03813-8.

13. Gouwens NW, Sorensen SA, Berg J, Lee C, Jarsky T, Ting J, et al. Classification of electrophysiological and morphological neuron types in the mouse visual cortex. Nat Neurosci. 2019 Jul;22(7):1182-95. Available from: https://dx.doi.org/0.1038/s41593-019-0417-0.

14. Bakken TE, Jorstad NL, Hu Q, Lake BB, Tian W, Kalmbach BE, et al. Comparative cellular analysis of motor cortex in human, marmoset, and mouse. Nature. 2021 Oct;598(7879):111-9. Available from: https://dx.doi.org/10.1038/s41586-021-03465-8.

15. Kalmbach BE, Buchin A, Long B, Close J, Nandi A, Miller JA, et al. h-Channels contribute to divergent intrinsic membrane properties of supragranular pyramidal neurons in human versus mouse cerebral cortex. Neuron. 2018 Dec;100(5):1194-205.e5. Available from: https://dx.doi.org/10.1016/j.neuron.2018.10.012.

16. Balint L, Braescu S, Kaslik E. Regions of attraction and applications to control theory. Cambridge Scientific Publishers Ltd; 2008. Edited by Sivasundaram S.

17. Hodgkin AL, Huxley AF. A quantitative description of membrane current and its application to conduction and excitation in nerve. J Physiol. 1952;117:500-44.

18. Weinberg SH. Membrane capacitive memory alters spiking in neurons described by the fractional order Hodgkin-Huxley model. PLoS One. 2015;10(5):e0126629. Available from: https://dx.doi.org/10.1371/journal.pone.0126629.

19. Balint AM, Balint S, Szabo R. Mathematical description of the ion transport across biological neuron membrane and in biological neuron networks, voltage propagation along neuron axons and dendrites, which use temporal classic Caputo or Riemann-Liouville fractional partial derivatives, is non-objective. MESA. 2021;12(4).

20. Curie J. Recherches sur le pouvoir inducteur spécifique et sur la conductibilité des corps cristallisés. Ann Chim Phys. 1889;17:384-434.

21. Curie J. Recherches sur la conductibilité des corps cristallisés. Ann Chim Phys. 1889;18:203-69.

22. Schweidler ER. Studien über die Anomalien im Verhalten der Dielektrika. Ann Phys. 1907;329(14):711-70. doi:10.1002/andp.19073291407.

23. Cojocaru AV, Balint S. Are power laws similar to constitutive laws? Can it be incorporated in the same way in the existing equations, boundary conditions, and initial conditions describing real-world phenomena? Is this a way to avoid temporal fractional-order derivatives? MESA.